

Design and research of suspended coal slurry concentration detection system based on photoelectric method

Houbao Huang, Jin Bo Zhu, Wei Zhou, Zilei Wang, Lingling Wang

School of Materials Science and Engineering, Anhui University of Science and Technology, Huainan 232001, China

Corresponding author: houbao_h@163.com (Houbao Huang)

Abstract: To address the inefficiencies and significant inaccuracies of conventional coal slurry water concentration detection methods in coal preparation plants, a detection device utilizing a photoelectric approach has been developed. This device employs photoelectric sensors, temperature sensors, and a microcontroller unit (MCU) to measure the voltage of the slurry water, subsequently calculating the corresponding concentration value through a mathematical model that correlates the concentration of coal slurry water with the sensor output voltage. The research findings indicate that the concentration detection system can identify concentration signals in real time, incorporating data processing, software calibration, and temperature adjustment functionalities. The detecting system can precisely measure the concentration of coal slurry water within the range of 0-20 g/L. The concentration detection gadget operates and is cost-effective to produce, addressing the limits of conventional detection methods while enhancing the efficiency and automation of coal selection.

Keywords: coal slurry water treatment, photoelectric sensor, concentration detection, online detection, photoelectric method, voltage value

1. Introduction

The processing of coal slurry water in the thickener is a crucial aspect of coal beneficiation plant operations. The concentration of coal slurry water within the thickener is vital; excessively high concentrations at the bottom can result in increased thickener load and potential rake pressure failures. Accurate coal slurry water concentration detection is significant for enhancing production efficiency and minimizing pharmaceutical consumption. The overflow water in the thickener can serve as circulating water to facilitate closed-circuit recycling of water resources during coal beneficiation, thereby alleviating the washing burden and enhancing flotation efficiency in mineral processing. Consequently, precise detection of the concentration of coal slurry water in the thickener's overflow layer is critically significant as a production guide. Currently, numerous techniques exist for measuring overflow water concentration, including the concentration pot method, ultrasonic measurement method (Yang et al., 2023; Tian 2014; Zhu and Lu, 2019), and CCD measurement method (Liu et al., 2023), among others. The practical application reveals that these established approaches include several deficiencies, including measuring data latency and imprecise or incorrect outcomes (Chen et al., 2014). Alongside traditional detection methods, recent research, including differential pressure methods (Lin et al., 2022), capacitance methods (Zhang et al., 2023), box pull pressure sensor detection (Zhang et al., 2022), and image processing detection methods (Sun et al., 2024), also faces challenges related to high equipment requirements, inadequate technological capabilities, and insufficient anti-jamming abilities. Current photoelectric technology is in the theoretical stage of development to a fairly mature stage and has started to be tried and applied in all areas of life. However, photoelectric technology is still in the exploration stage of development when it comes to the detection of liquid concentrations, where it primarily uses the principle of light transmission and scattering (Sheng et al., 2019). Although liquid turbidity detection devices have been developed (Kong et al., 2015) and the photoelectric detection method suggested in this paper has been used to detect water turbidity (Li et al., 2016; Li et al., 2020), the measurement's turbidity range is limited and cannot meet the technical requirements of determining

the concentration of coal slurry water (Yu et al., 2022). The concentration of suspended solids in a liquid exhibits a complex correlation with turbidity; typically, an increase in concentration results in heightened turbidity. However, it is essential to consider the nature of the substances, particle size, distribution, and other physicochemical properties of the water (Shi et al., 2022). The study demonstrates that the application of the photoelectric method in concentration detection yields commendable results (Zhao et al., 2024; Wu 2023; Deng et al., 2017). This study developed a photoelectric sensor and, utilizing a self-researched sensor integrated with a microcontroller, designed a real-time online detection device for coal slurry water concentration. The system thoroughly explored detection schemes and employed high-precision constant-current sources to drive the light source, incorporating key technologies such as I/V conversion and temperature compensation for signal acquisition, enabling high-precision measurements of coal slurry water across a wide range.

2. System detection principle

2.1. Concentration measurement principle

The fundamental idea of the system design relies on an infrared-to-tube photoelectric sensor, with the primary component being an infrared-to-tube circuit that includes an infrared diode and a photodiode. The concentration of two-phase flow is measured using an IR-to-tube photoelectric sensor, with the two-phase flow acting as a medium between the two diodes. Fig. 1 illustrates the IR-to-tube photoelectric sensor, comprising an infrared light-emitting diode (IR), a photodiode (PT), and the distance (L) between the two diodes. The Lambert-Beer law establishes a significant relationship between the size of a substance, its concentration, and the thickness of the liquid layer concerning light absorption. This fundamental principle applies to all electromagnetic radiation and light-absorbing substances.

$$I_T = I_0 \exp(-\alpha TL) \quad (1)$$

where: I_0 is the incident light intensity; I_T is the transmitted light intensity; α is the attenuation coefficient; T is a coefficient related to the solution concentration; L is the transmitted light range.

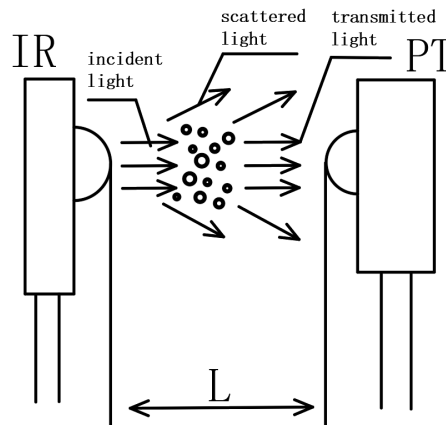


Fig. 1. Infrared to tube photoelectric sensor schematic diagram

Experiments indicate that light absorption by a solution correlates with the concentration of suspended particulate matter, the optical layer thickness, and the wavelength of the light source. The absorption effect is only dependent on the concentration of the solution when the wavelength of the light source and the optical path of the beam through the solution are held constant (Zhu et al., 2024). Assuming the solution to be analyzed is a homogeneous medium when the light source emits a beam with an incident light intensity of I_0 through the solution, the light intensity detected by the photosensitive sensor diminishes to I_T due to the absorption and scattering by suspended particulate matter, adhering to the Lambert-Beer absorption law.

Coal slurry water constitutes a solid-liquid two-phase flow, with its infrared light attenuation coefficient defined as $\epsilon_{\text{off}} = \alpha T$, where ϵ_a represents the attenuation coefficient of the solid and ϵ_b denotes the attenuation coefficient of the liquid. Given that the solid and liquid are thoroughly mixed,

the equivalent attenuation coefficients of the solid-liquid two-phase flow are contingent upon the volumes of both phases and the equivalent infrared light attenuation coefficient ϵ_{off} can be articulated as follows:

$$\epsilon_{\text{off}} = \frac{V_a}{V} \epsilon_a + \frac{V_b}{V} \epsilon_b \quad (2)$$

where: V_a is the volume of solid phase; V_b is the volume of liquid phase; V is the total volume of solid-liquid two-phase flow in the detected part.

Equation (2) can be derived as follows:

$$\epsilon_{\text{off}} = \frac{V_a}{V_a+V_b} \epsilon_a + \frac{V_b}{V_a+V_b} \epsilon_b = \epsilon_b + \frac{V_a}{V} (\epsilon_a - \epsilon_b) = k_1 \frac{V_a}{V} + b \quad (3)$$

Equation (3) demonstrates that the equivalent attenuation coefficient exhibits a linear functional connection with the volume fraction of the solid phase, where k_1 represents the linear function coefficient and b denotes the intercept.

Let the solid phase mass-volume concentration be C , i.e:

$$C = \frac{M_a}{V} = \rho \frac{V_a}{V} \quad (4)$$

where: M_a is the solid phase mass; ρ is the solid phase density.

By integrating Eq. (3) and Eq. (4), one may ascertain the infrared light attenuation coefficient, ϵ_{off} , as a function of the solid phase volume concentration C :

$$\epsilon_{\text{off}} = k_1 \frac{C}{\rho} + b \quad (5)$$

Equation (5) demonstrates that the equivalent attenuation coefficient exhibits a linear functional relationship with the mass-volume concentration of the solid phase at a specific density of the solid phase.

In the sensor of this study, the transmitted light intensity I_T is transformed into a current signal, designated as I_{in} , by the photodiode, which exhibits a linear response in converting the photoelectric signal. Subsequently, the current produced by the sensor is output through the operational amplifier as a voltage value V_{out} . It may be inferred that the output voltage and the intensity of the transmitted light exhibit a linear functional relationship.

$$V_{\text{out}} = k_2 I_T \quad (6)$$

where: k_2 Coefficient of a linear function of voltage value and intensity of transmitted light.

By integrating Eq. (1), Eq. (5), and Eq. (6), it can be inferred that an exponential relationship exists between the solid phase concentration and the measured voltage.

$$V_{\text{out}} = k_2 I_0 e^{-(k_1 \frac{C}{\rho} + b)L} \quad (7)$$

The constants k_1 , k_2 , I_0 , ρ , b and L pertain to the characteristics of the solid phase. From equation (7), the concentration of the solid phase in the coal slurry water can be determined by measuring the voltage value V_{out} .

2.2. Concentration detection program

The photoelectric sensor comprises a pair of infrared diode circuits and an operational amplifier circuit powered by an external 5V supply. In the circuit design, the infrared light-emitting diode and photodiode were connected in parallel with a 105 capacitor to facilitate voltage stabilization, filtering, denoising, and transient response. The infrared light-emitting diode is arranged in series with two resistors, R_1 and R_2 , along with a variable resistor to limit the current. The photodiode is linked in parallel to a trans-impedance amplifier circuit, which converts the current signal from the photodiode into a voltage signal and amplifies the output. The circuit architecture is illustrated in Fig. 2.

The constructed circuit exhibits no current traversing the operational amplifier inputs; hence, the currents from R_4 to R_3 are equivalent, and the currents from R_6 to R_7 are also equivalent.

$$\frac{V_1 - V_3}{R_4} = \frac{V_3 - V_{\text{out}}}{R_5} \quad (8)$$

$$\frac{V_2 - V_4}{R_6} = \frac{V_4}{R_7} \quad (9)$$

Owing to the virtual short characteristic of operational amplifiers, it is established that V_3 and V_4 are equivalent, so there exists:

$$V_3 - V_4 = 0 \quad (10)$$

The configured circuit features $R_4=R_6=10K$ and $R_3=R_7=12K$. By integrating Eq. (8), Eq. (9), and Eq. (10), the sensor's output voltage may be determined as follows: $0 \leq V_{out} \leq 4.8V$.

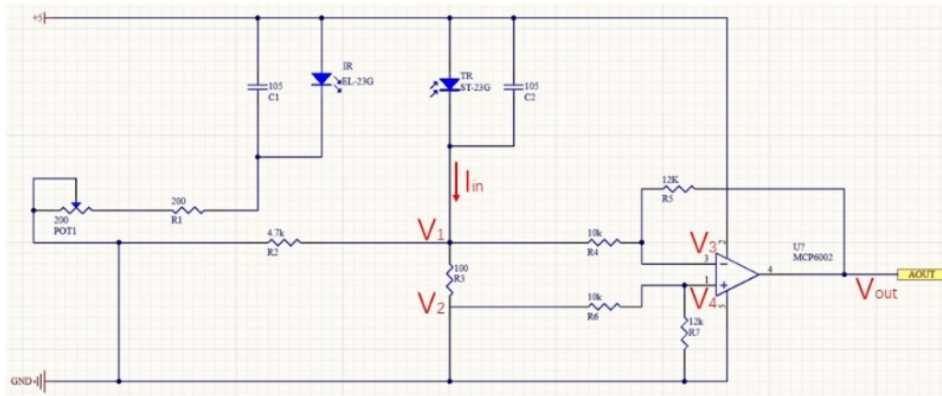


Fig. 2. Photoelectric sensor circuit design a photodiode exposed to varying light intensity can generate currents between 0 and 40 mA. $I_{in} = 0\sim 40mA$

3. Hardware Design

3.1. Hardware design program

The photoelectric concentration detection device comprises an infrared tube circuit, an operational amplifier circuit, an AD conversion circuit, and a temperature compensation circuit, forming the detection module. The microcontroller serves as the core, while the key circuit functions as a complementary control module. The display module includes an LCD screen and other peripherals. These three primary modules work synergistically and are powered by an external 5V power supply. The current produced by the infrared pair tube circuit is routed to the microcontroller's IO port via the AD conversion circuit following amplification by the operational amplifier. The temperature sensor is directly interfaced with the microcontroller's serial port. The microcontroller will process and compute the electrical signals from both the concentration sensor and the temperature sensor through software, ultimately displaying the concentration value on the LCD screen. The hardware design schematic of this system is illustrated in Fig. 3.

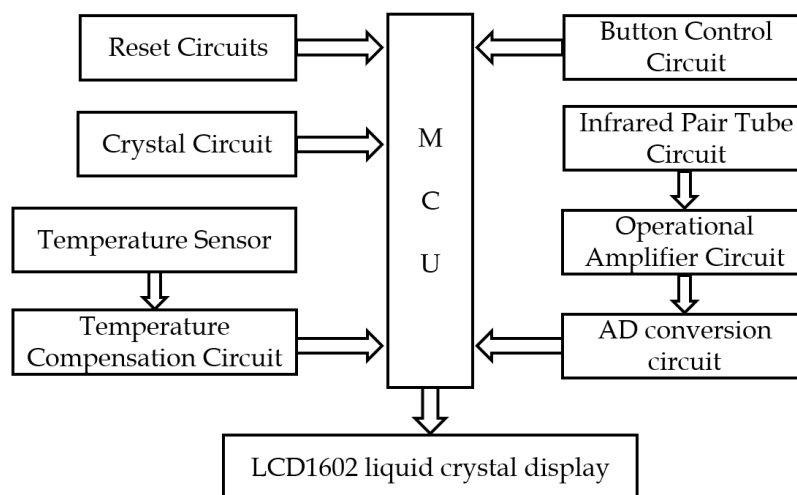


Fig. 3. Hardware design solutions

By thoroughly examining the detection scheme and anti-interference capabilities, the system employs a high-precision constant-current source to power the light source. It incorporates essential

technologies such as I/V conversion and temperature compensation for signal acquisition, enabling high-precision measurements of coal slurry water across an extensive range.

3.2. Detection module design

This study developed a novel sensor structure to quantify the concentration of coal slurry water. The design of the concentration detection device sensor structure is illustrated in Fig. 4. Fig. (a) depicts the infrared pair tube circuit PCB board, while (b) presents a three-dimensional model of the sensor's protective casing, which accommodates the PCB circuit board within the sensor shell. The complete sensor casing is constructed from transparent resin via 3D printing, exhibiting superior light transmittance. To mitigate external ambient light interference, the exterior of the casing is coated with black masking paint, and the entire casing is sealed with waterproof adhesive at the junction to safeguard the circuit components from damage.

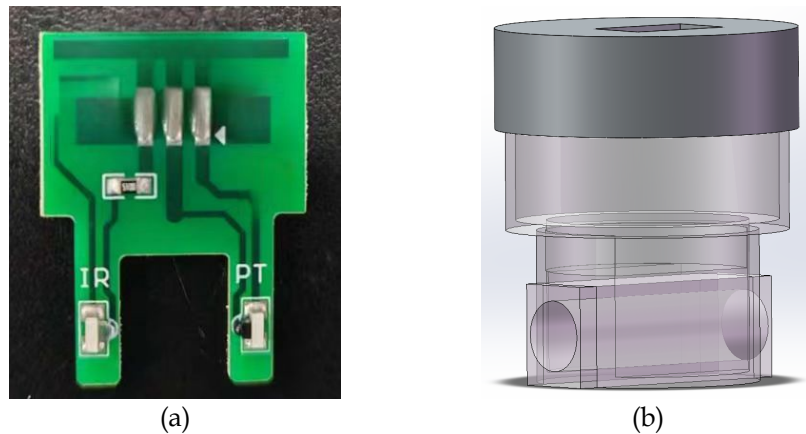


Fig. 4. Concentration sensor structure design

This research selects the South Korean photodiode EL-23G as the light source for the concentration detection system, which requires stability and longevity. The photodiode has a peak wavelength of 850nm and is situated in the near-infrared spectrum, effectively minimizing the impact of liquid chromaticity on concentration measurements. The light source is powered by a high-precision constant current circuit, ensuring the stability of the incident light intensity. The selected photodiode is the company's ST-23G diode, as the electrical signal provided by the photodiode is often weak, commonly at the mA level, necessitating the selection of an appropriate operational amplifier for I/V conversion. Operational amplifier circuit utilizing the MCP6002 model, AD conversion circuit employing the ADC0832 chip model, effective suppression of common mode interference to assure detection accuracy. To guarantee the measurement accuracy of the detection system across varying temperature environments, it is essential to implement temperature compensation for the sensor. The DS18B20 temperature sensor will be employed to measure the temperature of the liquid, with the temperature data transmitted via the serial port to the microcontroller for software-based temperature compensation. Upon testing, the temperature sensor exhibits commendable linearity, high sensitivity, and an accuracy of 0.1 °C, thereby satisfying the requirements for temperature compensation. Utilizing the sensor ensures that the liquid to be measured flows through or remains in the detecting column situated between the two diodes, enabling real-time online monitoring of the liquid's concentration.

3.3. Control module design

The system control chip utilizes the STC89C51 series microcontroller, incorporating a crystal circuit, reset circuit, and power supply circuit to establish the minimum system, together with a key circuit to constitute the control module of the entire system, as illustrated in Fig. 5. The crystal circuit comprises a 12MHz quartz crystal oscillator and two 30pF capacitors linked to the XTAL1 and XTAL2 terminals of the microcontroller, facilitating the generation of a 12MHz clock pulse signal within the microcontroller. In contrast, the capacitors contribute to rapid oscillation and frequency stabilization.

The reset circuit employs a key reset mechanism, comprising a 10kΩ resistor in series with a 10μF capacitor, with a pushbutton switch linked in parallel across the capacitor, enabling automatic system reset upon activation of the pushbutton switch. The pushbutton circuit is linked to the microcontroller's serial ports P2.2, P2.3, and P2.4, conFig.d to activate at a low level. The functions of the three pushbuttons are designated as the setup key, plus key, and minus key, respectively. The power supply circuit employs a design for constant voltage and current stabilization, while the rectifier filter circuit and switching conversion circuit guarantee the stability of the external 5V power supply voltage input.

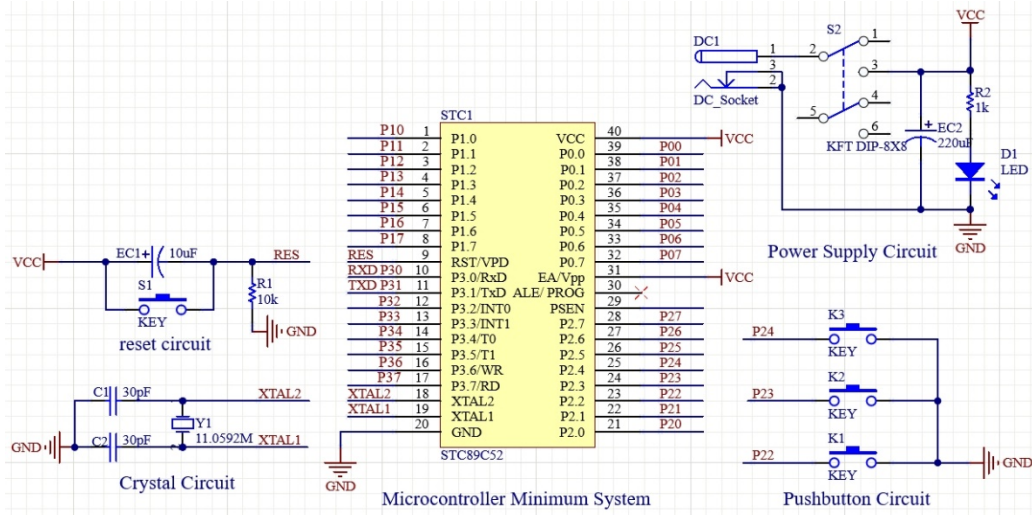


Fig. 5. Control module circuit design

3.4. Display module design

The LCD1602 display module is a highly reliable, low-power, and long-lasting character-type LCD widely utilized in various applications. It operates on a 5V output from a microcontroller and features a backlight. The module can display two lines of data, with each line accommodating 16 characters. It includes 192 built-in characters and 64 bytes of customizable character RAM. Communication is facilitated through a 4-bit or 8-bit parallel port, with the data and control terminals connected to P0.0 to P0.7, P2.5, P2.6, and P2.7, respectively. The communication interface is a 4-bit or 8-bit parallel port, with the LCD1602 data and control terminals linked to the microcontroller at P0.0 to P0.7, and P2.5, P2.6, P2.7 for the serial port. The LCD1602 display presents the concentration data detected by the sensor on the first line. In contrast, the second line exhibits the sensor's output voltage and the temperature data collected by the temperature sensor, as illustrated in Fig. 6. Furthermore, the primary circuit may regulate the system to modify the measurement range. By pressing the setup key, the LCD display reveals the concentration and temperature detection ranges, which can be altered in real-time using the plus and minus keys. When the concentration or temperature of the solution surpasses the established detection range, the system's buzzer will promptly emit an alarm.

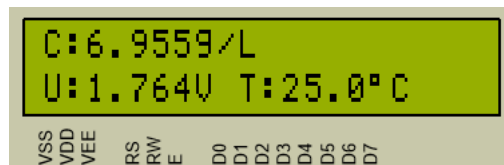


Fig. 6. Display module schematic

4. Software Development

4.1. Control process design

This system's software design uses C programming language and utilizes Keil uVision5. The program design is segmented into five components, mostly focusing on the core program design. The display program is designed in LCD1602.c, the key program in key.c, the temperature sensor program in

ds18b20.c, and the digital-analog conversion program in ADC.c. The system initiates the entire program via a switch key. Initially, the voltage data detected by the photoelectric sensor is transmitted to the microcontroller chip following digital-to-analog conversion. Concurrently, the temperature data is acquired from the temperature sensor. Subsequently, the software processes the data, calculating the concentration value from the voltage. Ultimately, the concentration, temperature, and voltage data are presented on the LCD1602 liquid crystal display. Fig. 7 illustrates the progression of the software design program.

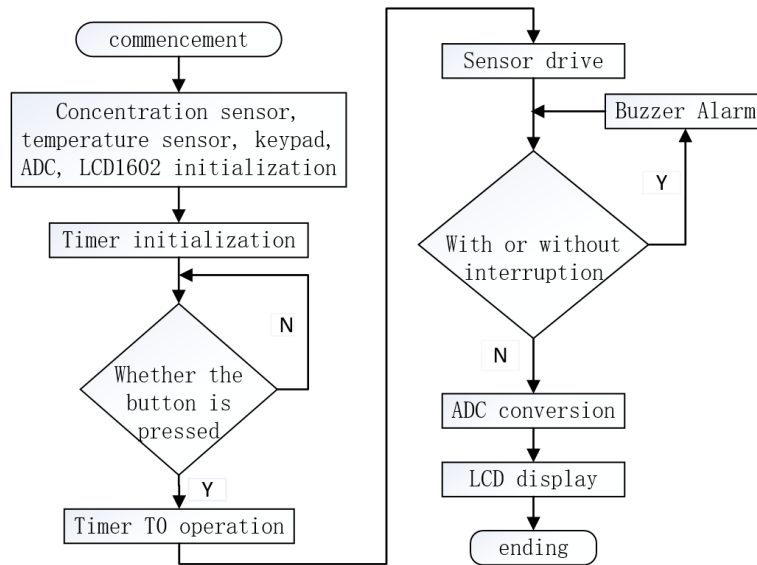


Fig. 7. Software design solution flowchart

4.2. Proteus simulation

Upon finalizing the hardware circuit and software program design of the system, it is essential to utilize Proteus software for system simulation. Utilizing Proteus, components are added in accordance with the schematic diagram, ensuring proper placement and connection of connections. The circuit for each module is represented in an engineering diagram, with the simulation engineering diagram illustrated in Fig. 8. The written C program is ultimately translated to .hex format and uploaded to the simulation project, allowing the project to be executed for simulation. Upon completion of debugging, the entire system operates with stability.

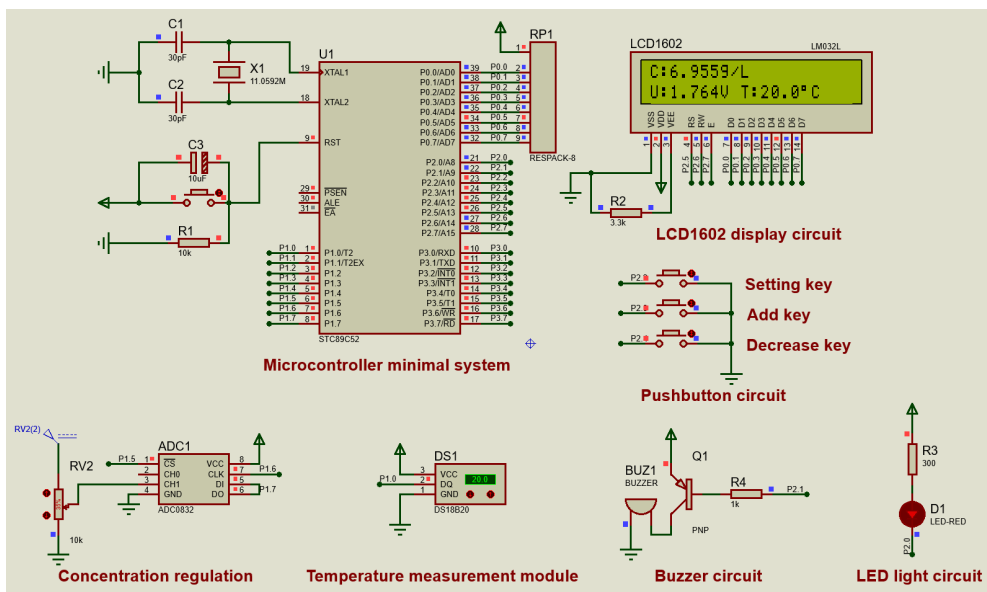


Fig. 8. Proteus simulation engineering drawing

5. Coal slurry water concentration testing experiment

The Proteus simulation has been finalized, and the device has been physically manufactured based on the circuit schematic designed with Altium Designer software. Subsequently, PCB circuit boards were produced, and electronic components were soldered. The completed physical device underwent initial power-on debugging to ensure the detection device's effective measurement capabilities. Calibration experiments were designed and conducted to ascertain concentration levels, followed by comparative verification experiments and analysis. To guarantee the detecting device's efficacy in measurement, develop and execute concentration calibration experiments, comparative verification experiments, and analytical experiments.

5.1. Concentration calibration experiment

The unprocessed coal was sieved, pulverized, and dried to produce experimental coal samples with a particle size of less than 0.5 mm. The coal samples were weighed using an electronic balance, with each group ranging from 1g to 20g, increasing by 1g for 20 groups. The experimental dry coal slurry density was $1.4\text{g}/\text{cm}^3$, indicating that the volume of each 1g of dry coal is approximately 0.7mL. Dry coal slurry was added to a concentration of $(1000-0.7n)$ mL of water in a specialized test bucket, where n represents the grams of dry coal. A total of 20 groups of coal slurry with known concentrations of the aqueous solution were prepared. Measure 10 liters of water using a measuring cylinder and transfer it into a 76-1A glass thermostatic water bath. Adjust the thermostatic temperature to 20°C and wait for the temperature to reach the designated value. Place the designated test bucket containing coal slurry water at the specified concentration into the thermostatic water bath until the solution reaches 20°C . Set the NP-40LS cantilever electric stirrer to a speed of 300 r/min and activate the stirrer for 3 minutes to ensure that the coal slurry particles are uniformly and completely suspended in the water. Cease stirring and allow the mixture to remain undisturbed for 5 seconds until the liquid in the barrel becomes static. At this point, the sensor is inserted into the turbidity detection barrel for a measurement duration of 5 seconds. Record the data if the measurement value displayed on the LCD screen stabilizes. Repeat this procedure five times to obtain voltage data and calculate the average value. The experimental data is illustrated in Fig. 9.

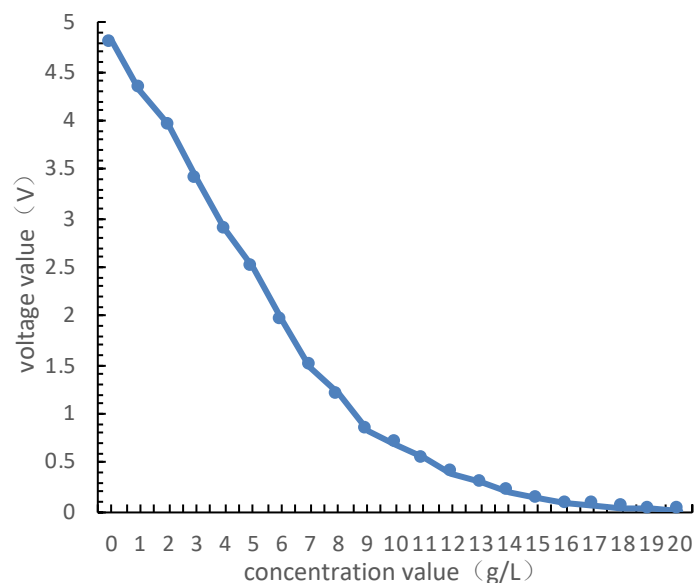


Fig. 9. Plot of concentration values versus mean voltage values

The data indicates that as the concentration of coal slurry water rises, the voltage value correspondingly declines. The rationale for this is that the coal slurry concentration per unit volume of water escalates, resulting in increased scattering of infrared light by the medium, diminished transmitted light, reduced light intensity detected by the photodiode, decreased output current, and a lower voltage registered by the system.

It is evident from the curve change in Fig. 9 that when measuring lower concentration samples using the photoelectric method, the data will be impacted by the slight change of the impurities in the samples to the results because of the properties of light decay in the propagation process. Consequently, internal contaminants can be eliminated prior to measurement or considered a component of the coal slurry water in real-world application scenarios when a lower concentration of coal slurry water is detected.

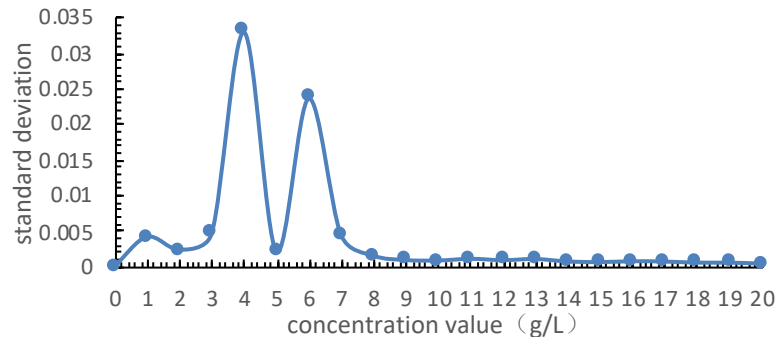


Fig. 10. Standard deviation of voltage values for different concentrations

Fig. 10 displays the standard deviation of the voltage data for five observations of each coal slurry water concentration. It is evident that in the great majority of instances, the standard error of the measured voltage value is less than 0.01; in a very tiny percentage of situations, the data error is little bigger but still falls within an acceptable range. As a result, the overall concentration detection system has outstanding stability and the measurement error of the photoelectric sensor is minimal.

The experimental data indicate an exponential relationship between coal slurry water concentration and measured voltage. Using Python for exponential function fitting, the mathematical model is illustrated in Fig. 11, and the functional relationship is expressed as follows:

$$y = 5.2695e^{-0.181x} \quad (11)$$

where: x is the concentration of coal slurry water, g/L; y is the voltage value, V.

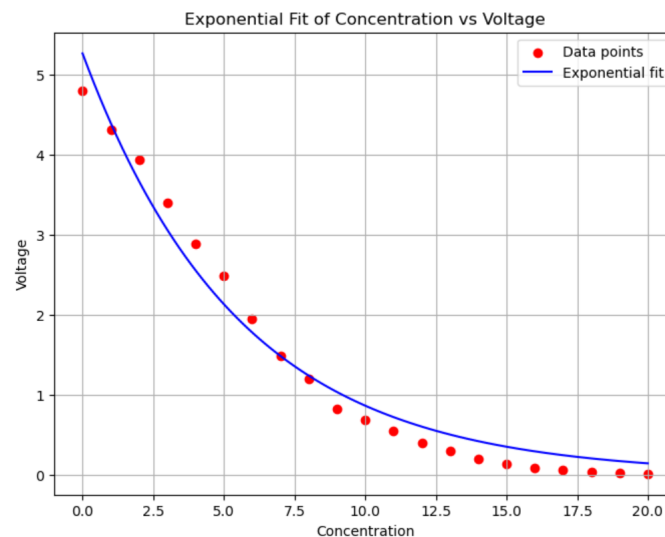


Fig. 11. Mathematical modeling of concentration and voltage

The calculated goodness-of-fit R^2 score and mean square error (MSE) of this functional equation are 0.9779 and 0.0530, respectively. The error is minimal, and it can serve as a mathematical model correlating the concentration of the coal slurry water with the measured voltage. The inverse function of this model serves as the conversion formula for voltage and concentration in subsequent experiments, implemented in C language, allowing the concentration value of coal slurry water to be displayed in

real-time on the device's LCD screen. The mathematical model's functional relationship is expressed as follows:

$$y = -\frac{\ln\left(\frac{x}{5.2695}\right)}{0.181} \quad (12)$$

where: x is the voltage value, V ; y is the concentration of coal slurry water, g/L .

The coal slurry water concentration was determined using the exponential function model fitted in Python, which showed a more pronounced difference at various but similar concentrations and a more stable exponential linear relationship. The sensitivity was computed for the low concentration zone with a slope, and the voltage declines nonlinearly with increasing concentration, which is consistent with the exponential decay feature (the high concentration zone converges to the baseline):

$$\left|\frac{dy}{dx}\right|_{x=0} = A \cdot B = 5.2695 \times 0.181 \approx 0.9538V/(g/L) \quad (13)$$

In other words, for every 1 g/L rise in voltage in the low concentration zone, the response value dropped by roughly 0.9538 V .

The sensitivity LOD and LOQ analyses were computed using five measurements at the maximum concentration (20 g/L) with a standard deviation of $\sigma = 0.0008366$ V . Blanket noise (σ) and LOD/LOQ calculations were carried out for the high concentration zone. The outcomes were:

$$LOD = \frac{3 \times \sigma}{\left|\frac{dy}{dx}\right|_{x=0}} = \frac{3 \times 0.0008366}{1.176} \approx 0.0021 \text{ g/L} \quad (14)$$

$$LOQ = \frac{10 \times \sigma}{\left|\frac{dy}{dx}\right|_{x=0}} = \frac{10 \times 0.0008366}{1.176} \approx 0.0071 \text{ g/L} \quad (15)$$

The suggested linear range was 0~15 g/L , and the analytical calculations demonstrated that the logarithmic transformation satisfied $R^2 > 0.99$ in the linear condition range. The linearization of logarithms was dependable. The method's detection capabilities were much enhanced after being refined by the exponential model, making it appropriate for the precise analysis of samples with low concentrations.

5.2. Comparative validation experiments

The concentration pot method is the prevalent method for measuring coal slurry water concentration in coal preparation plants. This is an indirect measurement technique wherein the density of the coal slurry and the mass of the coal slurry water are initially measured, followed by the indirect calculation of the coal slurry water concentration. To compare these two measuring methods, ten experimental groups were conducted, and the specific procedures of the experiments were as follows: Initially, the electronic scale was calibrated to zero, and the weight of the concentration pot was recorded. Subsequently, 1g, 3g, 5g, 7g, 9g, 11g, 13g, 15g, 17g, and 19g of dry coal slurry were sequentially measured. The density of the dry coal slurry for the experiments was consistently 1.4g/cm³. The concentration pot's overflow spout released a small quantity of coal slurry water until the flow ceased. The overflow spout was then covered, and the exterior of the concentration pot was wiped clean with a rag before weighing. The data was recorded, and the concentration value was calculated using the formula associated with the concentration pot method, noting that the empty pot weighed 100 g. Weigh 1g, 17g, and 19g of dry coal slurry, then sequentially transfer them into the 500mL concentration vessel, gradually adding water.

Subsequently, sequentially weigh 1g, 3g, 5g, 7g, 9g, 11g, 13g, 15g, 17g, and 19g of dry coal slurry, transferring each amount into a 500mL concentration pot and filling it with water. Agitate the coal slurry mixture to prevent sedimentation, and after achieving uniformity and stabilization, employ the homemade photoelectric sensor to measure the voltage value, recording the data sequentially. Finally, compute the concentration value using formula (12).

The theoretical real value of the concentration from the ten tests was calculated, followed by a comparison of the measured data from the photoelectric method and the concentration pot method, resulting in the data comparison table presented in Table 1.

The data presented in Table I indicate that the average relative errors for the concentration pot and photoelectric methods are 5.16% and 0.94%, respectively. Thus, the photoelectric method for measuring coal slurry water concentration not only facilitates rapid, real-time, and fully automated detection but

also demonstrates superior measurement accuracy compared to the traditional concentration pot method. It is evident that the software and hardware of the photoelectric sensing have good stability and accuracy because the measured data and calculated results data of the photoelectric method in Table 1 show that the results calculated using the calibration curves are essentially the same as the combination of measurements using the photoelectric sensors.

Table 1. Comparison table of experimental data

Coal /g	1	3	5	7	9	11	13	15	17	19
theoretical actual value (g/L)	0.50	1.50	2.50	3.50	4.50	5.50	6.50	7.50	8.50	9.50
concentration pot method (g/L)	0.53	1.61	2.66	3.72	4.75	5.80	6.74	7.81	8.76	9.85
photoelectricity method (g/L)	0.51	1.53	2.54	3.52	4.51	5.55	6.57	7.53	8.52	9.54
calculation result (g/L)	0.51	1.53	2.54	3.52	4.51	5.55	6.57	7.53	8.52	9.54

5.3. Analytical inquiry experiment

To conduct additional experiments on the concentration measurement of coal slurry water for this detection system, a vibrating sieve machine will be employed to classify the dry coal slurry into various particle size categories. The concentration measurement experiments will primarily focus on six particle sizes: 0.25–0.5 mm, 0.125–0.25 mm, 0.075–0.125 mm, 0.045–0.075 mm, and less than 0.045 mm. The dry coal slurry for each particle size was evaluated following the experimental procedures outlined in section 4.1. Coal samples of five distinct particle sizes were prepared, resulting in 100 groups of aqueous coal slurry solutions with known concentrations. Each group of samples underwent five repetitions, and the average of the five experimental results was computed. The experimental data for dry coal slurry of various particle sizes were represented on a single graph, with the concentration versus voltage for each particle size illustrated in Fig. 12.

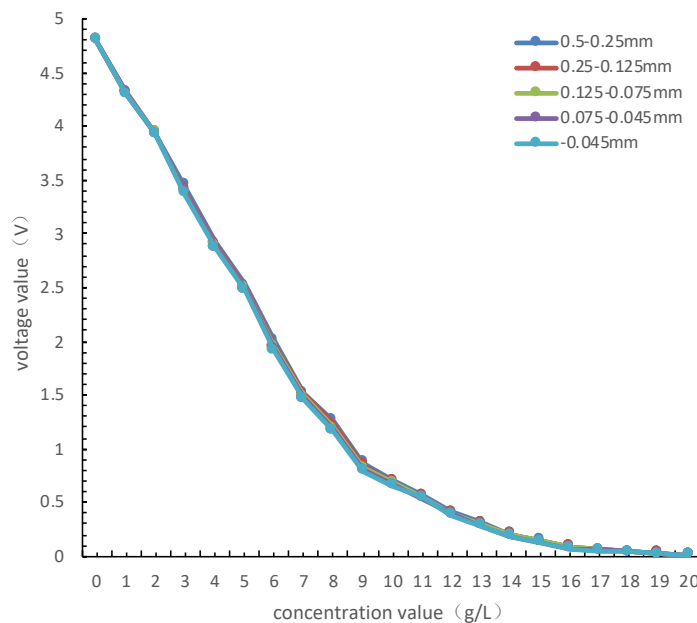


Fig. 12. Plot of coal slurry water concentration versus voltage for different particle size classes

The standard deviation of the coal slurry water measurements for various particle-size dry coal slurry configurations at each concentration was computed, and the results are presented in Fig. 13. The standard deviation of the coal slurry water concentration measurements for each particle size at identical concentrations is below 0.05.

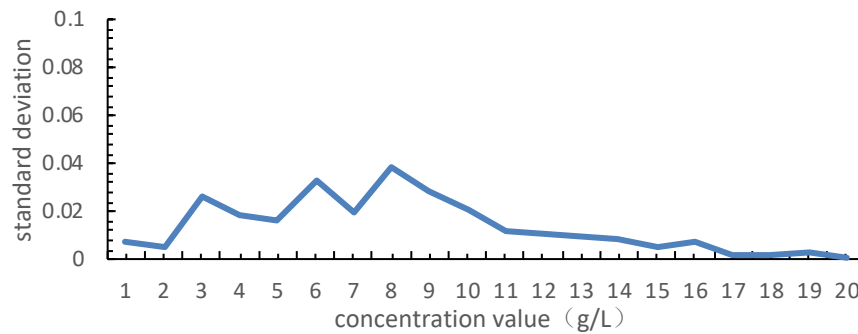


Fig. 13. Standard deviation of voltage values at each particle size level for different concentrations of coal slurry water

The data presented in Fig. 12 and Fig. 13 indicate that the voltage measurements obtained from coal slurry water, made from coal of varying particle sizes, exhibit greater consistency when analyzed using the photoelectric method, as evidenced by a reduced standard deviation. The impact of coal slurry particle size under 0.5mm on the concentration of coal slurry water, as measured by the photoelectric method, is minimal and negligible.

Additional tests were conducted to confirm the impact of chemicals on the concentration of coal slurry water detected by the photoelectric method. To do this, dry coal slurry with mixed particle sizes was used to create various concentrations of coal slurry water. Chemicals with varying molecular weights were then added to create experimental samples, which were then compared to the samples that were chemical-free. In order to compare samples of coal slurry water without additives, three groups of ten different concentrations of coal slurry water were first set up. Polyacrylamide is the primary flocculant used in coal slurry settlement, and in this experiment, 8 million molecular weight and 15 million molecular weight polyacrylamide solution were added to the coal slurry water. The experimental results are displayed in Table 2.

Table 2. Comparison table of experimental data of additive chemicals

Coal /g	1	3	5	7	9	11	13	15	17	19
Add 8 million molecular weight agents (g/L)	0.52	1.53	2.54	3.53	4.52	5.55	6.57	7.53	8.53	9.55
Add 15 million molecular weight agents(g/L)	0.52	1.53	2.54	3.54	4.53	5.55	6.57	7.54	8.53	9.55
No additives (g/L)	0.51	1.53	2.54	3.52	4.51	5.54	6.56	7.53	8.52	9.54

Using the photoelectric method, the results of adding 8 million molecular weight, 15 million molecular weight polyacrylamide solution, and coal slurry water without additives are essentially the same, as shown in Table 2. The very slight variation in data is primarily caused by the systematic error, indicating that the additives have very little effect on the photoelectric method's ability to detect the concentration of coal slurry water. Because the flocculant dissolves in water rather than being suspended in it, and because the resulting solution is transparent, light propagation has very little effect on the solution. The basic idea behind using it to settle coal slurry water is to adsorb the coal slurry and increase the flocs of the coal slurry in order to produce the effect of rapid sedimentation.

6. Conclusions

This study developed a high-precision, real-time online detection system for measuring the concentration of coal slurry water in concentration pools, utilizing a photoelectric method. A novel detection scheme was designed, with a microcontroller serving as the core for control and computation.

Infrared light detection was employed to assess the suspended solids content in the coal slurry water, measuring the intensity of transmitted light to obtain voltage data, from which the concentration of coal slurry water is inferred. The experiment demonstrates that the device achieves real-time online detection, offers straightforward operation, and incurs low production costs. The system immediately measures and displays the concentration of coal mud water, exhibiting good data accuracy and stability with minimal error.

References

- CHEN J., SHANG H., LING Y., et al., 2024. *Influence mechanism of Fe³⁺ doping on the hydrophobic regulation of kaolinite/water interface: Experiments and MD simulations*. *International Journal of Mining Science and Technology*, 4(11), 1575-1586.
- CHEN J., ZHANG Q., YANG L., 2014. *Current status and development trend of coal slurry water concentration detection*. *Coal Technology*, 33(11), 253-255.
- DENG J., ZHANG X., LIN Z., et al., 2017. *Research on automatic dosing system of coal slurry water based on photoelectric measurement*. *Clean Coal Technology*, 23(2), 92-97+102.
- KONG C., WANG Z., CHANG J., 2015. *Design and realization of photoelectric turbidity meter based on stm32 microcontroller*. *Journal of Jiangsu Second Normal College*, 31(3), 13-17, 124.
- LI X., CHEN Y., JIANG J., et al., 2016. *Estimation and analysis of suspended sand concentration based on turbidimeter and ADCP*. *Marine Science*, 40(6), 89-94.
- LI Z., GUO J., DING S., et al., 2020. *Design of water turbidity detection system based on stm32 for optical transmission method*. *Optical Instruments*, 42(2), 80-86.
- LIN X., LIU H., LU W., et al. 2022. *Design of coal slurry water concentration detection system based on differential pressure method*. *Shanxi Coking Coal Science and Technology*, 46(3), 34-36.
- LIU D., HOU Z., HU B., et al. 2023. *Measurement method of dust concentration surface dimension distribution based on ccd image*. *Journal of Heilongjiang University of Science and Technology*, 33(1), 99-102.
- SHENG B., YIN B., YU J., 2019. *Design of turbidity detection system based on scattering method and transmission method*. *Mechanical and Electrical Engineering*, 36(8), 771-776.
- SHI Z., ZHU H., OU Y., ZHUO M., et al., 2022. *Study on the relationship between suspended solids concentration and turbidity of Han River raw water in Wuhan*. *China Water Supply and Drainage*, 38(21), 51-56.
- SUN M., LV Z., XU Z., et al., 2024. *Utilizing spatio-temporal feature fusion in videos for detecting the fluidity of coal water slurry*. *International Journal of Mining Science and Technology*, 34(11), 1587-1597.
- TIAN J., 2014. *Research on ultrasonic detection technology of coal slurry water concentration*. China University of Mining and Technology (Beijing).
- WU R., 2023. *Application of online monitoring system of coal slurry water concentration and concentration gradient in thickener*. *Shanxi Coking Coal Science and Technology*, 47(2), 32-34.
- YANG X., LI B., QIAO S., 2023. *Design and application of ultrasound-based technology for detecting the concentration of coal slurry water*. *China Coal*, 49(10), 88-94.
- YU K., DONG Z., GU M., 2022. *Research on water quality monitoring system based on stm32*. *Jiangsu Science and Technology Information*, 39(17), 46-49.
- ZHANG L., LIU H., LU W., 2023. *Design of coal slurry water concentration detection device based on capacitance method*. *Shanxi Coking Coal Science and Technology*, 47(11), 26-29, 51.
- ZHANG Q., LIU H., LI Z., et al. 2022. *Real-time detection system of suspended solids concentration in thickening pond based on membrane cartridge tension sensor*. *Coal Technology*, 41(9), 239-242.
- ZHAO J., ZHANG W., ZHANG X., 2024. *Design and realization of turbidity transmitter with temperature compensation*. *Value Engineering*, 43(3), 101-103.
- ZHU Z., LU Y., 2019. *Ultrasonic sensing technology of coal slurry water deposition interface in coal concentrator of coal preparation plant*. *Clean Coal Technology*, 25(5), 162-166.
- ZHU Z., ZHAO B., TIAN C., et al., 2024. *Plasma pretreatment to enhance the sedimentation of ultrafine kaolinite particles: Experiments and mechanisms*. *Journal of Water Process Engineering*, 59105012.